

# Activation by IKK $\alpha$ of a Second, Evolutionary Conserved, NF- $\kappa$ B Signaling Pathway

Uwe Senftleben,<sup>1,2</sup> Yixue Cao,<sup>1</sup> Gutian Xiao,<sup>3</sup> Florian R. Greten,<sup>1</sup> Gertraud Krähn,<sup>1,4</sup> Giuseppina Bonizzi,<sup>1</sup> Yi Chen,<sup>1</sup> Yinling Hu,<sup>1</sup> Abraham Fong,<sup>3</sup> Shao-Cong Sun,<sup>3</sup> Michael Karin<sup>1\*</sup>

In mammals, the canonical nuclear factor  $\kappa$ B (NF- $\kappa$ B) signaling pathway activated in response to infections is based on degradation of I $\kappa$ B inhibitors. This pathway depends on the I $\kappa$ B kinase (IKK), which contains two catalytic subunits, IKK $\alpha$  and IKK $\beta$ . IKK $\beta$  is essential for inducible I $\kappa$ B phosphorylation and degradation, whereas IKK $\alpha$  is not. Here we show that IKK $\alpha$  is required for B cell maturation, formation of secondary lymphoid organs, increased expression of certain NF- $\kappa$ B target genes, and processing of the NF- $\kappa$ B2 (p100) precursor. IKK $\alpha$  preferentially phosphorylates NF- $\kappa$ B2, and this activity requires its phosphorylation by upstream kinases, one of which may be NF- $\kappa$ B-inducing kinase (NIK). IKK $\alpha$  is therefore a pivotal component of a second NF- $\kappa$ B activation pathway based on regulated NF- $\kappa$ B2 processing rather than I $\kappa$ B degradation.

Mammals express five NF- $\kappa$ B transcription factors: RelA, RelB, c-Rel, NF- $\kappa$ B1, and NF- $\kappa$ B2 (1). Unlike the Rel proteins, NF- $\kappa$ B1 and NF- $\kappa$ B2 are synthesized as large precursors (p105 and p100, respectively) that require proteolytic processing to produce their respective p50 and p52 NF- $\kappa$ B subunits (1). Mature NF- $\kappa$ B dimers are kept in the cytoplasm through interaction with inhibitory I $\kappa$ B proteins, and the major pathway leading to their activation is based on inducible I $\kappa$ B degradation (1, 2). This canonical pathway, triggered by proinflammatory cytokines, microbes, and viruses, requires activation of the IKK complex (2). Because the NF- $\kappa$ B1 and NF- $\kappa$ B2 precursors contain I $\kappa$ B-like ankyrin repeats in their COOH-termini, they can function as I $\kappa$ Bs (3, 4). Unlike I $\kappa$ B degradation, processing of NF- $\kappa$ B1 is a constitutive process (5, 6). NF- $\kappa$ B2 processing, however, could be a regulated process because it is most active in mature B cell lines (7) and is defective in *aly* mice (8). The *aly* mutation, which maps to the gene encoding NIK, interferes with the development of primary and secondary lymphoid organs (9), as does a complete NIK deficiency (10). Interestingly, NIK induces ubiquitin-dependent processing of NF- $\kappa$ B2 (11) but is not required for induction of NF- $\kappa$ B DNA binding activity (12).

NIK was discovered as an NF- $\kappa$ B-activating kinase (12) and was later shown to phos-

phorylate and activate IKK $\alpha$  (13), one of the two catalytic subunits of the IKK complex (2). The other catalytic subunit, IKK $\beta$ , is 52% identical to IKK $\alpha$  (2), and in vitro both subunits exhibit I $\kappa$ B kinase activity (14). Despite these similarities, IKK $\alpha$  and IKK $\beta$  have distinct functions (2, 5). IKK $\beta$  is essential for proper activation of NF- $\kappa$ B in response to proinflammatory stimuli and for prevention of tumor necrosis factor (TNF- $\alpha$ )-induced apoptosis (15–18), whereas IKK $\alpha$  is dispensable for IKK activation and induction of NF- $\kappa$ B DNA binding activity in most cell types (17, 19). IKK $\alpha$ , but not IKK $\beta$ , is essential for proper skeletal morphogenesis and differentiation of the epidermis (19, 20). However, this function does not depend on IKK activity or NF- $\kappa$ B activation (21). These findings raise the question of whether IKK $\alpha$  has any NF- $\kappa$ B-related functions that are masked by the perinatal lethality of *Ikk $\alpha$ <sup>-/-</sup>* mice. Here, we provide evidence that IKK $\alpha$  kinase activity is required for B cell maturation, formation of secondary lymphoid organs, induction of a subset of NF- $\kappa$ B target genes, and inducible NF- $\kappa$ B2 processing. This function of IKK $\alpha$  is strikingly similar to that of *Drosophila* IKK, which is required for processing of Relish, a NF- $\kappa$ B2-like precursor protein (22, 23). In addition to explaining the function of IKK $\alpha$ , these results shed new light on the mechanisms involved in the evolution of innate and adaptive immunity.

Analysis of bone marrow cells from wild-type, *Ikk $\alpha$ <sup>-/-</sup>*, and *Ikk $\beta$ <sup>-/-</sup>* radiation chimeras (24) revealed complete absence of B cells in *Ikk $\beta$ <sup>-/-</sup>*-derived samples (25). By contrast, B cells were present in *Ikk $\alpha$ <sup>-/-</sup>* reconstituted bone marrow (25). Although these cells expressed normal levels of early B cell markers, a B220<sup>hi</sup>CD24<sup>lo</sup> population, representing circulating mature B cells, was absent (25). No differences in absolute numbers of thymo-

ing the amygdala were excised from 40- $\mu$ m-thick vibratome sections and fixed in 4% paraformaldehyde and 0.1% glutaraldehyde in PBS. After fixation with OsO<sub>4</sub>, tissue samples for routine electron microscopy were embedded in epoxy resin (Epon, Sigma, Bornem, Belgium). For immunogold labeling, ultrathin sections from epoxy resin-embedded tissues on formvar-coated nickel grids were treated with 6% sodium metaperiodate for 10 min and with 5% normal goat serum in PBS for 30 min. This was followed by incubating the sections with monoclonal antibody AT8 in 1% normal goat serum in PBS at a dilution of 1:50 for 2 hours. After washing, 10-nm colloidal gold-tagged secondary antibody in tris-buffered saline (goat anti-mouse; British Biocell, Cardiff, UK) was applied for 1 hour. Then, after washing, sections were stained with lead citrate and uranyl acetate. Control sections were stained following the same procedure, but with omission of the primary antibody. AT8 appeared to label frequently "ends" of filaments because filaments sectioned at the surfaces of the epoxy-embedded preparations were more easily accessible to the antibodies than were deeper layers.

14. M. G. Spillantini et al., *Am. J. Pathol.* **153**, 1359 (1998).
15. S. Varadarajan, S. Yatin, M. Aksanova, D. A. Butterfield, *J. Struct. Biol.* **130**, 184 (2000).
16. J. Lewis et al., *Science* **293**, 1487 (2001).
17. D. L. Price, S. S. Sisodia, *Annu. Rev. Med.* **45**, 435 (1994).
18. S. E. Arnold, B. T. Hyman, J. Flory, A. R. Damasio, G. W. Van Hoesen, *Cereb. Cortex* **1**, 103 (1991).
19. J. Götz, F. Chen, J. van Dorpe, R. M. Nitsch, data not shown.
20. I. Grundke-Iqbal et al., *Proc. Natl. Acad. Sci. U.S.A.* **83**, 4913 (1986).
21. H. Braak, E. Braak, *Neurobiol. Aging* **16**, 271 (1995).
22. G. A. Jicha, R. Bowser, I. G. Kazam, P. Davies, *J. Neurosci. Res.* **48**, 128 (1997).
23. M. Goedert et al., *Biochem. J.* **301**, 871 (1994).
24. D. W. Dickson et al., *Neurobiol. Aging* **16**, 285 (1995).
25. T. Tanaka, J. Zhong, K. Iqbal, E. Trenkner, I. Grundke-Iqbal, *FEBS Lett.* **426**, 248 (1998).
26. S. G. Greenberg, P. Davies, J. D. Schein, L. I. Binder, *J. Biol. Chem.* **267**, 564 (1992).
27. M. Goedert, R. Jakes, E. Vanmechelen, *Neurosci. Lett.* **189**, 167 (1995).
28. P. Seubert et al., *J. Biol. Chem.* **270**, 18917 (1995).
29. V. Buee-Scherrer et al., *Brain Res. Mol. Brain Res.* **39**, 79 (1996).
30. A. Delacourte, N. Sergeant, A. Watzek, D. Gauvreau, Y. Robitaille, *Ann. Neurol.* **43**, 193 (1998).
31. N. Sergeant, A. Watzek, A. Delacourte, *J. Neurochem.* **72**, 1243 (1999).
32. J. Gotz, A. Probst, E. Ehler, B. Hemmings, W. Kues, *Proc. Natl. Acad. Sci. U.S.A.* **95**, 12370 (1998).
33. J. Busciglio, A. Lorenzo, J. Yeh, B. A. Yankner, *Neuron* **14**, 879 (1995).
34. C. Geula et al., *Nature Med.* **4**, 827 (1998).
35. L. Buee, T. Bussiere, V. Buee-Scherrer, A. Delacourte, P. R. Hof, *Brain Res. Brain Res. Rev.* **33**, 95 (2000).
36. K. K. Hsiao et al., *Neuron* **15**, 1203 (1995).
37. A. Probst et al., *Acta Neuropathol. (Berlin)* **99**, 469 (2000).
38. We thank E. Moritz, D. Schuppli, B. Knecht, and H.-P. Gautschi for technical assistance and J. Opoku for animal care. We also thank P. Davies (Bronx, NY) for antibodies PHF1, TG3, and MC1; P. Seubert (Elan Pharmaceuticals, South San Francisco) for antibody 12E8; A. Delacourte for antiserum S199P; K. Iqbal for antibody R145d; and C. Mourton-Gilles (Lille, France) for antibody AD2. We thank T. Baechli for providing the electron microscopy facility and members of his laboratory for assistance, and M. Glatzel for suggesting the use of Texas red-coupled dextran. Supported by the University of Zürich and, in part, by grants from Evotec NeuroSciences, Bayer Pharma AG (BARN; Bayer Alzheimer's Disease Research Network), the Swiss National Foundation (SNF), and the National Center for Competence in Research (NCCR) "Neuronal Plasticity and Repair."

30 April 2001; accepted 11 July 2001

<sup>1</sup>Laboratory of Gene Regulation and Signal Transduction, Department of Pharmacology, University of California, San Diego, 9500 Gilman Drive, La Jolla, CA 92093, USA. <sup>2</sup>Clinic for Anesthesiology, University of Ulm, Steinhövelstrasse 9, 89075 Ulm, Germany. <sup>3</sup>Department of Microbiology and Immunology, Pennsylvania State University College of Medicine, Hershey, PA 17033, USA. <sup>4</sup>Department of Dermatology, University of Ulm, Oberer Eselsberg 40, 89081 Ulm, Germany.

\*To whom correspondence should be addressed.

cytes and peripheral T cell populations were found between wild-type and *Ikkα*<sup>-/-</sup> radiation chimeras (25). This is in marked contrast to *Ikkβ*<sup>-/-</sup> radiation chimeras, which lack B and T cells (18). Analysis of B cell markers in *Ikkα*<sup>-/-</sup> reconstituted spleen and lymph nodes revealed a reduction of the mature IgM<sup>lo</sup>IgD<sup>hi</sup> population (Ig, immunoglobulin) relative to virgin IgM<sup>hi</sup> B cells (Fig. 1A). Whereas the splenic B to T cell ratio was almost normal 6 weeks after reconstitution with *Ikkα*<sup>-/-</sup> stem cells, it was considerably reduced thereafter, mostly as a result of the loss of mature IgM<sup>lo</sup>IgD<sup>hi</sup> B cells (25). This defect in B lymphopoiesis is cell-autonomous (25).

Examination of B cell turnover by means of bromodeoxyuridine (BrdU) labeling (26) revealed that *Ikkα*<sup>-/-</sup> B cells incorporated more BrdU than did wild-type B cells (Fig. 1B). The high turnover of *Ikkα*<sup>-/-</sup> B cells is likely to account for the lower fraction of circulating mature B cells (Fig. 1A) and the lower frequency of mature IgD<sup>+</sup> B cells in *Ikkα*<sup>-/-</sup> lymph nodes (Fig. 1C). The increased turnover of *Ikkα*<sup>-/-</sup> B cells correlates with higher rates of spontaneous apoptosis, seen in vitro (Fig. 1D) and in vivo (25). *Ikkα*<sup>-/-</sup> B cells also exhibit

defective mitogenic responses to antibody to IgM and especially to lipopolysaccharide (LPS) (25). To test whether immune responses dependent on cellular interactions are functional, we immunized mice with dinitrophenol–keyhole limpet hemocyanin (DNP-KLH), and 12 days later we evaluated the formation of germinal centers (GCs) (27). Wild-type spleens exhibited numerous GCs characterized by B cell areas that bound peanut agglutinin (PNA). In contrast, the spleens of *Ikkα*<sup>-/-</sup> radiation chimeras contained very few PNA-stainable cells (Fig. 1E).

The absence of IKKα can be compensated by IKKβ in liver and keratinocytes, leading to normal IKK and NF-κB activation by proinflammatory stimuli (19, 21). Biochemical analysis of purified resting and stimulated B cells from radiation chimeras yielded similar results. Basal IKK activity was elevated in *Ikkα*<sup>-/-</sup> B cells (Fig. 2A). This was associated with lower IκBα levels and somewhat higher basal NF-κB DNA binding activity (Fig. 2B). However, no major differences in LPS-induced IKK and NF-κB DNA binding activities were detected between *Ikkα*<sup>+/+</sup> and *Ikkα*<sup>-/-</sup> B cells (Fig. 2, A and B). These results were highly reproducible and were seen upon analysis of at least five different pairs of radiation chimeras (25). We

also compared the expression of individual NF-κB proteins and found similar amounts of RelA, c-Rel, RelB, and NF-κB1 p105 and p50 (Fig. 2, C and D). Strikingly, however, *Ikkα*<sup>-/-</sup> B cells exhibited defective processing of NF-κB2 and contained very little p52 and increased amounts of p100 (Fig. 2D). These defects were observed in bone marrow, spleen, and lymph node–derived B cells, regardless of their NF-κB2 expression level.

Having found defective NF-κB2 processing in *Ikkα*<sup>-/-</sup> B cells, we examined whether NF-κB complexes in these cells were indeed deficient in p52. To optimize the detection of p52-containing NF-κB complexes, we used a palindromic NF-κB binding site (1) and an antibody capable of binding to such complexes. This analysis revealed smaller amounts of p52-containing NF-κB complexes in *Ikkα*<sup>-/-</sup> B cells (Fig. 2E).

To determine the role of IKKα phosphorylation by upstream kinases, such as NIK [which is also required for B cell maturation, GC formation, and NF-κB processing (8)], we generated *Ikkα*<sup>AA</sup> knock-in mice in which the activating phosphorylation sites of IKKα, Ser<sup>176</sup> and Ser<sup>180</sup>, were replaced by alanines (28). Although *Ikkα*<sup>AA</sup> mice are viable, we wished to

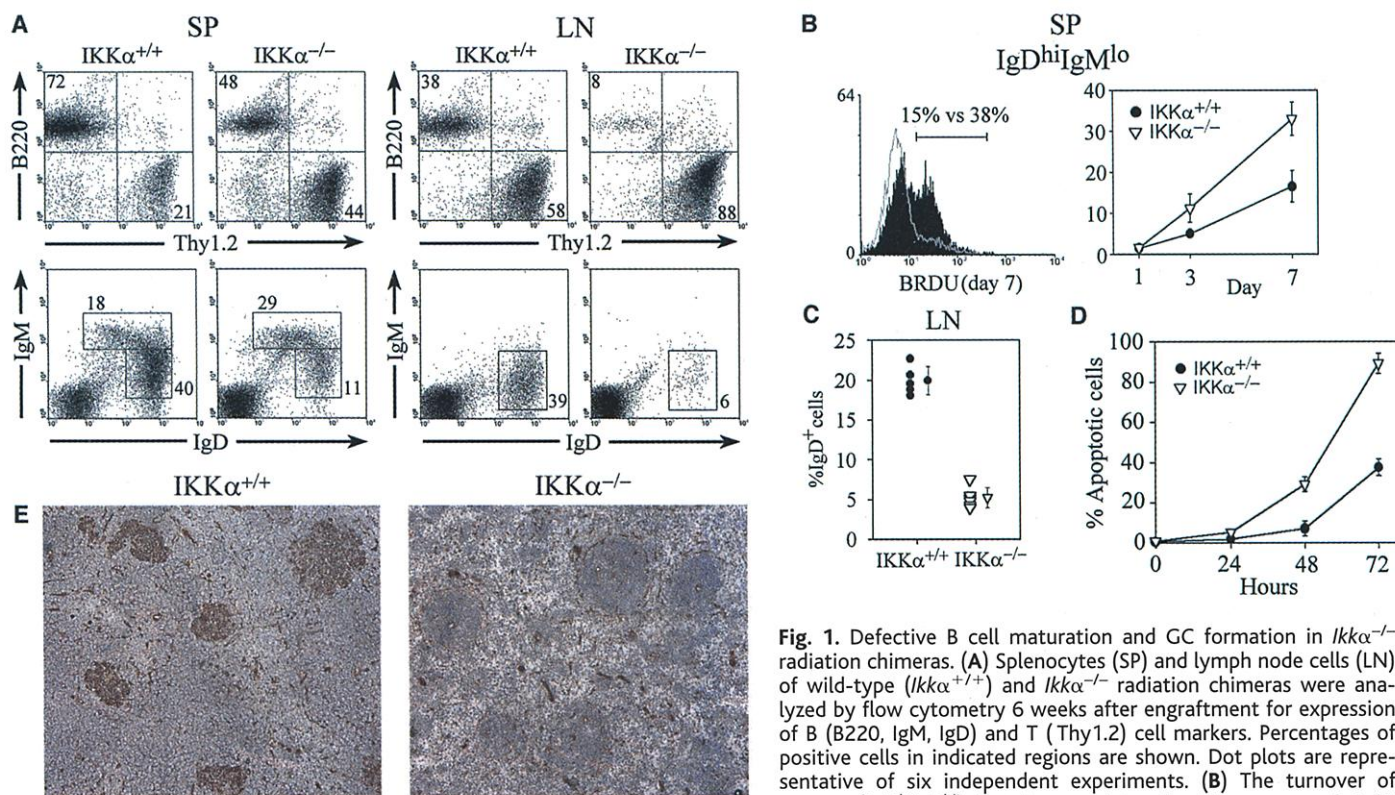


**Fig. 1.** Defective B cell maturation and GC formation in *Ikkα*<sup>-/-</sup> radiation chimeras. (A) Splenocytes (SP) and lymph node cells (LN) of wild-type (*Ikkα*<sup>+/+</sup>) and *Ikkα*<sup>-/-</sup> radiation chimeras were analyzed by flow cytometry 6 weeks after engraftment for expression of B (B220, IgM, IgD) and T (Thy1.2) cell markers. Percentages of positive cells in indicated regions are shown. Dot plots are representative of six independent experiments. (B) The turnover of mature (IgM<sup>lo</sup>IgD<sup>hi</sup>) B cells was determined by means of BrdU

incorporation. Eight weeks after engraftment, mice were administered BrdU and splenocytes (SP) were analyzed by flow cytometry after three-color staining for BrdU, IgM, and IgD. Left panel: BrdU incorporation into mature splenic B cells of *Ikkα*<sup>+/+</sup> (gray) and *Ikkα*<sup>-/-</sup> (black) radiation chimeras after 7 days of labeling. Right panel: Kinetics of BrdU incorporation over a 7-day period. Values represent means ± SD for three mice in each group and time point. (C) Frequencies of mature IgD<sup>+</sup> lymph node B cells in *Ikkα*<sup>+/+</sup> and *Ikkα*<sup>-/-</sup> radiation chimeras (*n* = 5 each group, mean ± SD). (D) CD43<sup>-</sup> resting splenic B cells were purified and cultured without stimulation for 72 hours. At 24-hour intervals, percentages of apoptotic cells were determined by 7-amino-actinomycin D staining. Initially, more than 97% of the cells were viable (*n* = 3 each group, mean ± SD). (E) *Ikkα*<sup>-/-</sup> and wild-type radiation chimeras were injected with DNP-KLH. After 12 days, their spleens were stained with PNA and counterstained with hematoxylin. Almost no GC formation could be detected in *Ikkα*<sup>-/-</sup> reconstituted spleens.

REPORTS

analyze the effect of this mutation on B cell development under the same conditions as the *Ikkα<sup>-/-</sup>* null mutation. We therefore generated *Ikkα<sup>AA</sup>* radiation chimeras and found a reduction in mature IgD<sup>+</sup> B cells in their spleens and lymph nodes (Fig. 3, A and B). However, a more pronounced deficiency of mature B cells was detected in untreated 12-week-old *Ikkα<sup>AA</sup>* mice (Fig. 3, A and B). In addition, untreated *Ikkα<sup>AA</sup>* mice lacked distinct Peyer's patches and exhibited defective GC formation after immunization with DNP-KLH (Fig. 3C). Defects found in *Ikkα<sup>AA</sup>* radiation chimeras were less severe (25). Untreated *Ikkα<sup>AA</sup>* mice also exhibited defective NF-κB2 processing in purified splenic and lymph node B cells, as well as in bone marrow B cells, which express smaller amounts of NF-κB2 (Fig. 3D). The reduction in NF-κB2 processing (~80%) was less severe than that caused by the complete IKKα deficiency. Although basal and LPS-induced NF-κB DNA binding activities were only slightly reduced in *Ikkα<sup>AA</sup>* cells (Fig. 3E), the relative amount of p52-containing NF-κB complexes was substantially decreased (Fig. 3F).

We also examined whether *Ikkα<sup>AA</sup>* B cells exhibit defective NF-κB-mediated gene induction. Splenic B cells were isolated from wild-type and *Ikkα<sup>AA</sup>* mice that were or were not injected with LPS, and expression of known NF-κB target genes was analyzed by real-time polymerase chain reaction (PCR) (29). Transcription of several NF-κB target genes, including those encoding cyclin D2 and TNF-α, was similarly increased in wild-type and *Ikkα<sup>AA</sup>* B cells, but expression of other target genes—including those for macrophage inflammatory protein (MIP)-1α and receptor activator of NF-κB (RANK) ligand—was clearly defective in *Ikkα<sup>AA</sup>* cells (Table 1). Thus, IKKα phosphorylation is also required for increased expression of a subset of NF-κB target genes in B cells.

In addition to autophosphorylation by IKK, Ser<sup>176</sup> and Ser<sup>180</sup> of IKKα can be phosphorylated by NIK (13). Like IKKα, NIK is required for NF-κB2 processing (8, 11). Although NIK overexpression was shown to stimulate NF-κB2 phosphorylation (11), the results described above suggested that NIK may act via IKKα. Currently, the only known activator of NIK is the lymphotoxin β receptor (LTβR), which is not expressed in B cells (10). We therefore resorted to a surrogate system based on cotransfection of NIK and NF-κB2 expression vectors into wild-type, *Ikkα<sup>-/-</sup>*, and *Ikkβ<sup>-/-</sup>* mouse fibroblasts. NIK induced NF-κB2 processing in wild-type and *Ikkβ<sup>-/-</sup>* cells, but not in *Ikkα<sup>-/-</sup>* cells (Fig. 4A). However, reexpression of IKKα in *Ikkα<sup>-/-</sup>* cells restored NIK's ability to induce NF-κB2 processing.

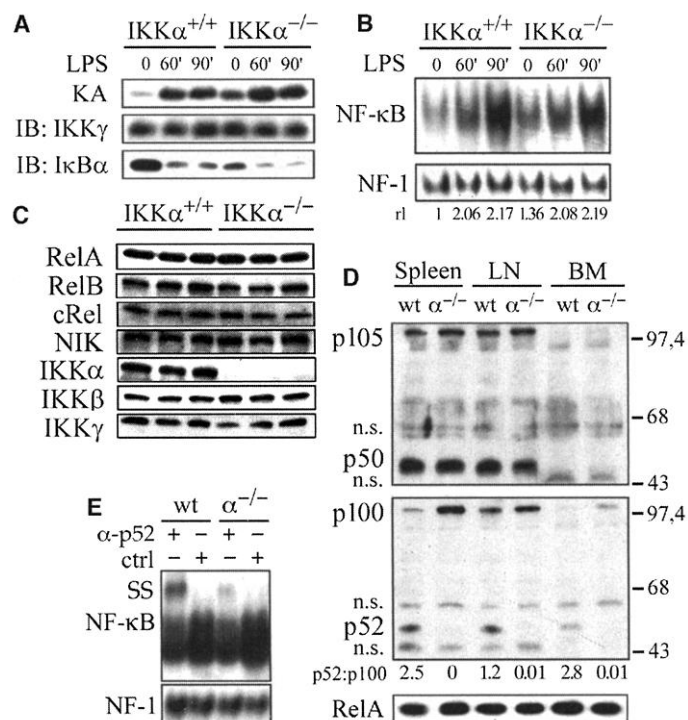
We also compared the abilities of recombinant NIK, IKKα, or IKKβ (14) to phosphorylate the regulatory domains of IκBα and NF-

κB2. IκBα was phosphorylated much more efficiently by IKKβ than by IKKα and not at all by NIK (Fig. 4B). The COOH-terminal regulatory domain of NF-κB2, however, was phosphorylated most efficiently by IKKα. This clear difference in substrate specificities between IKKα and IKKβ correlates with their different biological functions.

Previous experiments established the role of IKKβ in inducible IκB degradation and activa-

tion of NF-κB in response to infections and proinflammatory stimuli (15–18), but the role of IKKα in this process has remained enigmatic. Although not essential for the canonical NF-κB activation pathway, IKKα is required for proper patterning of the epidermis (19, 20), but this function is not mediated by IκB or NF-κB and does not require the kinase activity of IKKα (21). Our results demonstrate that IKKα is physiologically involved in NF-κB

**Fig. 2.** Normal NF-κB DNA binding but defective NF-κB2 processing in *Ikkα<sup>-/-</sup>* radiation chimeras. (A) Purified splenic B cells were stimulated with LPS (5 μg/ml). IKK activity and IκBα levels were determined at 0, 60, and 90 min, as indicated. IKK recovery was determined by immunoblotting (IB) with antibody to IKKγ. (B) NF-κB and NF-1 DNA binding activities in purified splenic B cells treated with LPS (5 μg/ml) were determined at 0, 60, and 90 min. Data in (A) and (B) are representative of at least five independent experiments; the average relative levels (rl) of NF-κB to NF-1 DNA binding activities in these experiments are indicated at the bottom of (B). (C) Expression of the indicated NF-κB proteins, NIK, and IKK subunits was examined by immunoblotting. Three individual wild-type and *Ikkα<sup>-/-</sup>* radiation chimeras were analyzed. (D) Splenic, lymph node (LN), and bone marrow (BM) B cells from groups of three *Ikkα<sup>+/+</sup>* (wt) and three *Ikkα<sup>-/-</sup>* (*α<sup>-/-</sup>*) radiation chimeras were pooled and analyzed by immunoblotting for expression of NF-κB1 (p105 and p50), NF-κB2 (p100 and p52), and RelA. Migration positions of molecular weight standards (in kilodaltons) are indicated at the right. (E) Splenic B cells were analyzed for p52-containing NF-κB complexes. Nuclear extracts from B cells pooled from three different wild-type and *Ikkα<sup>-/-</sup>* radiation chimeras were incubated with a palindromic NF-κB binding site in the presence of either anti-p52 (06-413, Upstate Biotechnology) or a control antiserum that does not recognize p52. Extract quality was monitored by binding to an NF-1 probe. SS, supershifted p52-containing complex.



(C) Expression of the indicated NF-κB proteins, NIK, and IKK subunits was examined by immunoblotting. Three individual wild-type and *Ikkα<sup>-/-</sup>* radiation chimeras were analyzed. (D) Splenic, lymph node (LN), and bone marrow (BM) B cells from groups of three *Ikkα<sup>+/+</sup>* (wt) and three *Ikkα<sup>-/-</sup>* (*α<sup>-/-</sup>*) radiation chimeras were pooled and analyzed by immunoblotting for expression of NF-κB1 (p105 and p50), NF-κB2 (p100 and p52), and RelA. Migration positions of molecular weight standards (in kilodaltons) are indicated at the right. (E) Splenic B cells were analyzed for p52-containing NF-κB complexes. Nuclear extracts from B cells pooled from three different wild-type and *Ikkα<sup>-/-</sup>* radiation chimeras were incubated with a palindromic NF-κB binding site in the presence of either anti-p52 (06-413, Upstate Biotechnology) or a control antiserum that does not recognize p52. Extract quality was monitored by binding to an NF-1 probe. SS, supershifted p52-containing complex.

**Table 1.** Analysis of NF-κB target gene expression in wild-type and *Ikkα<sup>AA</sup>* B cells. Wild-type and *Ikkα<sup>AA</sup>* mice were injected with LPS (5 mg/kg ip) or phosphate-buffered saline. After 1 or 4 hours, splenic B cells were isolated and their RNA was extracted. Expression of the indicated NF-κB target genes was analyzed by RealTime PCR (Taq Man, PE Applied Biosystems) and normalized to the level of cyclophilin mRNA (29). Reverse transcription was done with 2 μg of total RNA, followed by 40 PCR cycles at 95°C for 15 s and 60°C for 1 min (Sybr Green Core Reagents, PE Applied Biosystems). Primer sequences are available upon request. The values represent change in mRNA abundance relative to the untreated sample of each genotype and are averages of two fully separate experiments. iNOS, inducible nitric oxide synthase.

Genotype	Target							
	IκBα	TNF-α	NF-κB2	Cyclin D2	Bcl-2	MIP-1α	iNOS	RANK-L
WT, 1 hour	2.05	4.97	0.51	1.14	1.77	3.35	4.38	8.87
WT, 4 hours	1.87	2.78	1.07	5.45	1.14	2.01	2.20	3.26
<i>IKKα<sup>AA</sup></i> , 1 hour	0.80	3.37	1.18	1.58	0.76	0.73	0.44	0.28
<i>IKKα<sup>AA</sup></i> , 4 hours	0.85	2.06	1.31	5.77	0.83	0.80	0.44	0.11

REPORTS

regulation, but instead of doing so through inducible I $\kappa$ B degradation, it exerts at least some of its NF- $\kappa$ B-related functions by regulating

the processing of NF- $\kappa$ B2. Defective NF- $\kappa$ B2 processing in *Ikk $\alpha$ <sup>-/-</sup>* or *Ikk $\alpha$ <sup>AA</sup>* B cells is likely to interfere with their maturation and with the

formation of secondary lymphoid organs. A similar defect in B cell maturation was recently described by Kaisho *et al.* (30), who reconstituted *Rag2<sup>-/-</sup>* mice with *Ikk $\alpha$ <sup>-/-</sup>* stem cells. These authors attributed the defect to decreased NF- $\kappa$ B DNA binding activity in *Ikk $\alpha$ <sup>-/-</sup>* splenic B cells (30). However, we found a slight reduction in LPS-induced NF- $\kappa$ B DNA binding activity in *Ikk $\alpha$ <sup>AA</sup>* but not in *Ikk $\alpha$ <sup>-/-</sup>* B cells. Similarly, the absence or inactivation of NIK, which may act upstream to IKK $\alpha$ , does not affect total NF- $\kappa$ B DNA binding activity (10) but does inhibit NF- $\kappa$ B2 processing (8, 11). Both the absence of NIK (10) and the *Ikk $\alpha$ <sup>AA</sup>* mutation reduce the expression of certain NF- $\kappa$ B target genes.

Expression of NF- $\kappa$ B2 itself is increased in more mature B cell lines (7) and is up-regulated during B cell development (Figs. 2 and 3). However, no defect in NF- $\kappa$ B2 expression, other than its processing, was detected in IKK $\alpha$ -deficient B cells, regardless of their maturation state. Hence, the processing defect is not the consequence of defective B cell maturation. Although the complete knockout of the *Nf $\kappa$ b2* gene also results in lymphoid organ defects, including the absence of GCs (31), the effects are not identical to those of the *Ikk $\alpha$*  mutations, which exert a more severe effect on B cell development. However, the *Nf $\kappa$ b2<sup>-/-</sup>* mutation abolishes expression of both p100 and p52, whereas the *Ikk $\alpha$*  mutations reduce p52 and increase p100 expression. Congruently, the specific ablation of p100 in the presence of p52 expression results in increased lymphocyte proliferation and enlargement of spleen and lymph nodes (32).

NIK overexpression was shown to enhance NF- $\kappa$ B2 phosphorylation and processing (11). Our results strongly suggest that NIK acts via IKK $\alpha$ . First, the *Ikk $\alpha$ <sup>AA</sup>* mutation, which replaces the NIK phosphorylation sites of IKK $\alpha$  with alanines, inhibits NF- $\kappa$ B2 processing, B cell maturation, and formation of secondary lymphoid organs. Second, NIK fails to stimulate NF- $\kappa$ B2 processing in the absence of IKK $\alpha$ . Third, IKK $\alpha$  is more potent than NIK as a NF- $\kappa$ B2 COOH-terminal kinase. At this point it is not clear whether both NIK and IKK $\alpha$  phosphorylate the COOH-terminal regulatory domain of NF- $\kappa$ B2, or whether this activity is provided by IKK $\alpha$  alone, whose activation is NIK-dependent. NIK itself is thought to be activated by LT $\beta$ R, a member of the TNF receptor family (9, 10). Indeed, *Lt $\beta$ r<sup>-/-</sup>* mice exhibit defects similar to those of *aly* mice, which encompass those caused by the *Ikk $\alpha$ <sup>AA</sup>* mutation (33). However, LT $\beta$ R is expressed in the stroma but not in lymphoid cells, and therefore it cannot activate the NIK-IKK $\alpha$ -NF- $\kappa$ B2 pathway in lymphoid cells. Adoptive transfer experiments suggest that IKK $\alpha$  phosphorylation, like expression of NIK (8) or NF- $\kappa$ B2 (31), is also required outside the B cell com-

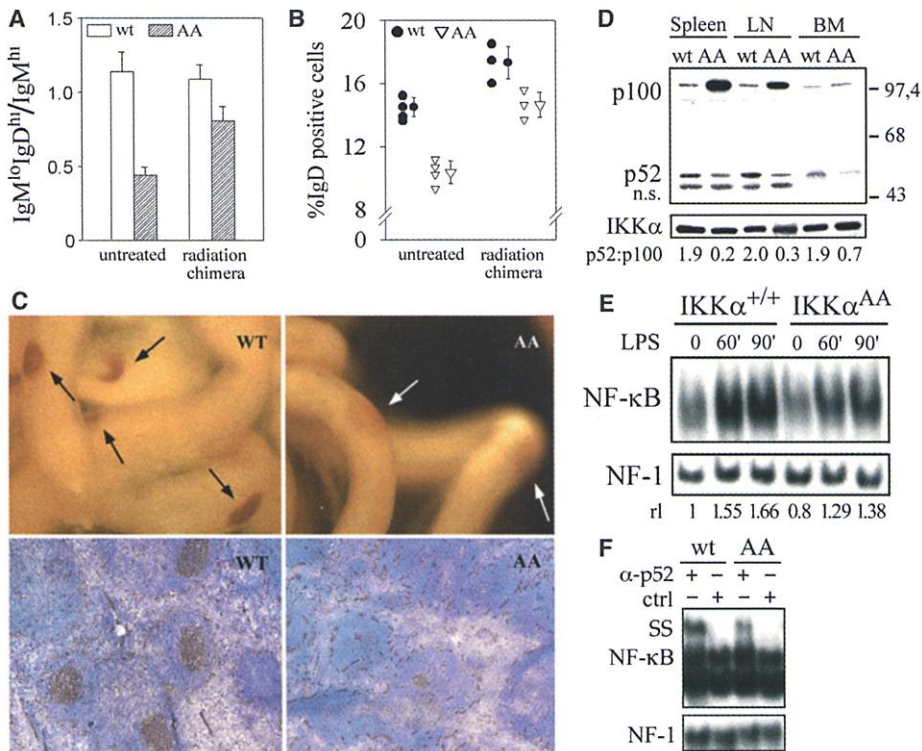


**Fig. 3.** Requirement of IKK $\alpha$  phosphorylation for B cell maturation and NF- $\kappa$ B2 processing. (A) The ratio of virgin (IgM<sup>hi</sup>) to mature (IgM<sup>lo</sup>IgD<sup>hi</sup>) splenic B cells in untreated wild-type (wt) and *Ikk $\alpha$ <sup>AA</sup>* (AA) mice and radiation chimeras was determined by flow cytometry. Data are means  $\pm$  SEM for three animals in each group. (B) Relative frequencies of mature IgD<sup>+</sup> lymph node B cells in untreated wild-type and *Ikk $\alpha$ <sup>AA</sup>* mice and radiation chimeras. (C) Peyer's patches (top panels) and GCs (bottom panels) in wild-type and *Ikk $\alpha$ <sup>AA</sup>* mice. Mice were immunized with DNP-KLH and examined 12 days later to assess GC formation. Peyer's patches (arrows) were visualized by staining with antibody to VCAM1. (D) Immunoblot analysis of NF- $\kappa$ B2 processing in purified B cells from spleen, lymph nodes, and bone marrow of untreated wild-type and *Ikk $\alpha$ <sup>AA</sup>* mice. The ratio of p52 to p100 is indicated at the bottom. IKK $\alpha$  levels were used to verify equal loading. Data are representative of three independent experiments. (E) Splenic B cells from *Ikk $\alpha$ <sup>+/+</sup>* and *Ikk $\alpha$ <sup>AA</sup>* mice were stimulated with LPS, and NF- $\kappa$ B and NF-1 DNA binding activities were determined. Average relative levels (rl) of NF- $\kappa$ B to NF-1 DNA binding activities in five such experiments are indicated at the bottom. (F) The content of p52-containing NF- $\kappa$ B complexes in splenic B cells was determined as described in (E).

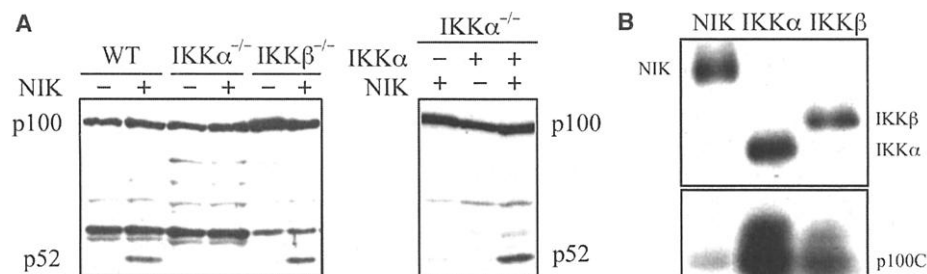


**Fig. 4.** Involvement of IKK $\alpha$  in NIK-induced NF- $\kappa$ B2 processing and NF- $\kappa$ B2 COOH-terminal phosphorylation. (A) Mouse fibroblasts derived from wild-type, *Ikk $\alpha$ <sup>-/-</sup>*, and *Ikk $\beta$ <sup>-/-</sup>* embryos were transfected with an NF- $\kappa$ B2 p100 expression vector with or without NIK and IKK $\alpha$  expression vectors. After 36 hours, the processing of NF- $\kappa$ B2 was examined by immunoblotting with an NH<sub>2</sub>-terminal-specific p100 antibody. (B) Chromatographically pure IKK $\alpha$  and IKK $\beta$  (50 ng each) and immunopurified NIK, all produced in Sf9 cells using baculoviruses, were examined for phosphorylation of GST-I $\kappa$ B $\alpha$ (1-54) and GST-NF- $\kappa$ B2(754-900)(p100C) fusion proteins (11, 14) as well as for autophosphorylation.

partment for formation of secondary lymphoid organs.

Our findings illustrate a novel function for IKK $\alpha$  that depends on its protein kinase activity and cannot be compensated by the related IKK $\beta$  subunit. Although both IKK catalytic subunits are involved in the activation of NF- $\kappa$ B transcription factors, they do so via different mechanisms and substrates. IKK $\beta$  is the canonical activator of NF- $\kappa$ B in response to infection and inflammation, and IKK $\alpha$  is responsible for activation of a specific NF- $\kappa$ B factor required for B cell maturation and formation of secondary lymphoid organs. This function is exerted through processing of NF- $\kappa$ B2 and is remarkably similar to the function of the *Drosophila* IKK complex, which contains a single catalytic subunit that is similar to both IKK $\alpha$  and IKK $\beta$  (22, 23). The DmIKK/Ird5 protein does not phosphorylate the single I $\kappa$ B of *Drosophila*, Cactus, and instead leads to activation of antibacterial genes through phosphorylation-induced processing of the *Drosophila* NF- $\kappa$ B1/2 homolog, Relish (22, 23). Although in *Drosophila* the processing-dependent NF- $\kappa$ B pathway is the major provider of innate antibacterial immunity (23), in mammals this pathway has been assigned to a specific aspect of adaptive immunity: B cell maturation and formation of secondary lymphoid organs. Thus, the duplication of IKK catalytic subunits and their functional divergence correlates with the evolution of the immune system.

References and Notes

1. S. Ghosh, M. J. May, E. B. Kopp, *Annu. Rev. Immunol.* **16**, 225 (1998).
2. D. M. Rothwarf, M. Karin, *Science's STKE*, [www.sciencemag.org/cgi/content/full/OC\\_sigtans;1999/5/re1](http://www.sciencemag.org/cgi/content/full/OC_sigtans;1999/5/re1) (26 October 1999).
3. N. R. Rice, M. L. Mackichan, A. Israel, *Cell* **78**, 773 (1992).
4. F. Mercurio, J. DiDonato, C. Rosette, M. Karin, *Genes Dev.* **7**, 705 (1993).
5. M. Karin, Y. Ben-Neriah, *Annu. Rev. Immunol.* **18**, 621 (2000).
6. L. Lin, G. N. DeMartino, W. C. Greene, *Cell* **92**, 819 (1998).
7. H. C. Liou, W. C. Sha, M. L. Scott, D. Baltimore, *Mol. Cell. Biol.* **14**, 5349 (1994).
8. T. Yamada *et al.*, *J. Immunol.* **165**, 804 (2000).
9. R. Shinkura *et al.*, *Nature Genet.* **22**, 74 (1999).
10. L. Yin *et al.*, *Science* **291**, 2162 (2001).
11. G. Xiao, E. W. Harhaj, S. C. Sun, *Mol. Cell* **7**, 401 (2001).
12. N. L. Malinin, M. P. Boldin, A. V. Kovalenko, D. Wallach, *Nature* **385**, 540 (1997).
13. L. Ling, Z. Cao, D. V. Goeddel, *Proc. Natl. Acad. Sci. U.S.A.* **95**, 2791 (1998).
14. E. Zandi, Y. Chen, M. Karin, *Science* **281**, 1360 (1998).
15. Q. Li, D. Van Antwerp, F. Mercurio, K.-F. Lee, I. M. Verma, *Science* **284**, 321 (1999).
16. Z.-W. Li *et al.*, *J. Exp. Med.* **189**, 1839 (1999).
17. W. M. Chu *et al.*, *Immunity* **11**, 721 (1999).
18. U. Senftleben, Z.-W. Li, V. Baud, M. Karin, *Immunity* **14**, 217 (2001).
19. Y. Hu *et al.*, *Science* **284**, 316 (1999).
20. K. Takeda *et al.*, *Science* **284**, 313 (1999).
21. Y. Hu *et al.*, *Nature* **410**, 710 (2001).
22. N. Silverman *et al.*, *Genes Dev.* **14**, 2461 (2000).
23. Y. Lu, L. P. Wu, K. V. Anderson, *Genes Dev.* **15**, 104 (2001).
24. Fetal livers were harvested from embryonic day 16

- wild-type, *Ikka*<sup>-/-</sup>, or *Ikka*<sup>AA</sup> embryos as described (18). Genomic DNA was genotyped using IKK $\alpha$ -specific primers (19). Single-cell suspensions were injected into the tail vein of lethally irradiated 8-week-old C57BL/6-CD45.1 female hosts (18). Mice were analyzed after 6 weeks or more. The donor origin of the analyzed cells was verified by CD45.2 staining (18).
25. See supplementary information at Science Online ([www.sciencemag.org/cgi/content/full/293/5534/1495/DC1](http://www.sciencemag.org/cgi/content/full/293/5534/1495/DC1)).
26. BrdU (Sigma) was administered for 7 days in the drinking water. DNA-incorporated BrdU was detected by flow cytometry after staining fixed (0.5% paraformaldehyde for 20 min) and permeabilized (3 N HCl and 0.5% Tween-20 followed by neutralization with 0.1 M disodium tetraborate) cells with a fluorescein-5-isothiocyanate-labeled antibody (BU-1, Becton Dickinson) in the presence of 0.5% Tween-20. B cells were marked by prestaining with anti-IgM (phycoerythrin-labeled R6-60.2, Pharmingen) and anti-IgD (11-26c.2a, Pharmingen) + anti-rat IgG [F(ab')<sub>2</sub>, TC, Caltag]. Bone marrow cells from untreated and BrdU-treated mice served as negative and positive controls, respectively.
27. Lymphoid organs were fixed in 10% buffered formalin and embedded in paraffin. Sections were stained with hematoxylin and eosin for histological analysis. TUNEL (terminal deoxynucleotidyl transferase-mediated deoxyuridine triphosphate nick-end labeling) staining was performed using the In Situ Cell Detection kit (Boehringer Mannheim). For analysis of GC formation, mice were injected intraperitoneally (ip) with 100 mg of DNP-KLH absorbed to alum (Calbiochem) and spleens were collected 14 days later. Cryosections were stained with biotinylated PNA (Vector Laboratories), incubated with streptavidin peroxidase (Jackson Immunoresearch) for 30 min, and developed with 3,3'-diaminobenzidine (DAB) kit (Leinco Technologies). Sections were counterstained with hematoxylin (Sigma). For visualization of

- Peyer's patches, intestines were fixed in 0.5% paraformaldehyde, rinsed, and dehydrated in a methanol series. Endogenous peroxidase was inactivated with H<sub>2</sub>O<sub>2</sub>. After rehydration and blocking, the tissue was stained with anti-VCAM1 (Pharmingen) followed by staining with a secondary goat antibody to rat IgG conjugated to horseradish peroxidase. After washing, the tissue was developed with DAB kit.
28. A targeting vector in which the codons for Ser<sup>176</sup> and Ser<sup>180</sup> in the activation loop of IKK $\alpha$  were replaced by alanine codons was used to construct the *Ikka*<sup>AA</sup> allele. Full description and characterization of this mutant will be provided elsewhere (34). *Ikka*<sup>AA</sup> mice are viable, fertile, and morphologically indistinguishable from wild-type mice.
29. U. E. Gibson, C. A. Heid, P. M. Williams, *Genome Res.* **6**, 995 (1996).
30. T. Kaisho *et al.*, *J. Exp. Med.* **193**, 417 (2001).
31. G. Franzoso *et al.*, *J. Exp. Med.* **187**, 147 (1998).
32. H. Ishikawa, D. Carrasco, E. Claudio, R. P. Ryseck, R. Bravo, *J. Exp. Med.* **186**, 999 (1997).
33. A. Futterer, K. Mink, A. Luz, M. H. Kosco-Vilbois, K. Pfeffer, *Immunity* **9**, 59 (1998).
34. Y. Cao *et al.*, in preparation.
35. We thank C. Surh for advice on radiation chimeras, R. Rickert for many helpful and critical discussions, M. Delhase and V. Baud for advice and assistance with IKK and NF- $\kappa$ B assays, M. Matsumoto for advice on detection of Peyer's patches, C. Adams for manuscript preparation, and G. Ghosh and E. Raz for comments. Supported by postdoctoral fellowships from the Deutsche Forschungsgemeinschaft (U.S., F.R.G.), California Breast Cancer Research Project (Y.C.), Human Frontier Science Program (G.B.), Arthritis Foundation (Y.H.), NIH (grants AI434477 and ESO4151 to M.K. and AI45045 to S.-C.S.), and the California Cancer Research Program. M.K. is an American Cancer Society Research Professor.

18 May 2001; accepted 3 July 2001

## Crystal Structure of Sensory Rhodopsin II at 2.4 Angstroms: Insights into Color Tuning and Transducer Interaction

Hartmut Luecke,<sup>1,2\*</sup> Brigitte Schobert,<sup>2</sup> Janos K. Lanyi,<sup>2\*</sup> Elena N. Spudich,<sup>3</sup> John L. Spudich<sup>3\*</sup>

We report an atomic-resolution structure for a sensory member of the microbial rhodopsin family, the phototaxis receptor sensory rhodopsin II (NpSRII), which mediates blue-light avoidance by the haloarchaeon *Natronobacterium pharaonis*. The 2.4 angstrom structure reveals features responsible for the 70- to 80-nanometer blue shift of its absorption maximum relative to those of haloarchaeal transport rhodopsins, as well as structural differences due to its sensory, as opposed to transport, function. Multiple factors appear to account for the spectral tuning difference with respect to bacteriorhodopsin: (i) repositioning of the guanidinium group of arginine 72, a residue that interacts with the counterion to the retinylidene protonated Schiff base; (ii) rearrangement of the protein near the retinal ring; and (iii) changes in tilt and slant of the retinal polyene chain. Inspection of the surface topography reveals an exposed polar residue, tyrosine 199, not present in bacteriorhodopsin, in the middle of the membrane bilayer. We propose that this residue interacts with the adjacent helices of the cognate NpSRII transducer NpHtrII.

Microbial rhodopsins are a family of membrane-embedded photoactive retinylidene proteins found throughout the three domains of life: archaea (1-3), eubacteria (4), and

unicellular eukaryotes (5, 6). They share a common design of seven transmembrane helices forming an interior pocket for the chromophore retinal, and their functions are driv-